MINOR, W., JANKOWSKI, M. & BOLIN, J. T. (1992). In preparation.
ROSSMANN, M. G. (1972). *The Molecular Replacement Method.* New York: Gordon & Breach.
ROSSMANN, M. G. (1990). *Acta Cryst.* A**46**, 73-82.
ROSSMANN, M. G. & BLOW, D. M. (1962). *Acta Cryst.* **15**, 24-31.
ROSSMANN, M. G., MCKENNA, R., TONG, L., XIA, D., DAI, J.-B., WU, H., CHOI, H.-K. & LYNCH, R. E. (1992). *J. Appl. Cryst.* **25**, 166-180.
SAPER, M. A., BJORKMAN, P. J. & WILEY, D. C. (1991). *J. Mol. Biol.* **219**, 277-319.
SHOPE, R. E. (1980). In *The Togaviruses. Biology, Structure, Replication*, edited by R. W. SCHLESINGER, pp. 47-82. New York: Academic Press.
TONG, L. & ROSSMANN, M. G. (1990). *Acta Cryst.* A**46**, 783-792.
VARGHESE, J. N., LAVER, W. G. & COLMAN, P. M. (1983). *Nature (London)*, **303**, 35-40.
WANG, B. C. (1985). *Methods Enzymol.* **115**, 90-112.
WANG, J., YAN, Y., GARRETT, T. P. J., LIU, J., RODGERS, D. W., GARLICK, R. L., TARR, G. E., HUSAIN, Y., REINHERZ, E. L. & HARRISON, S. C. (1990). *Nature (London)*, **348**, 411-418.

Acta Cryst. (1992). A**48**, 442-451

Parametrization of Triply Periodic Minimal Surfaces. I. Mathematical Basis of the Construction Algorithm for the Regular Class

BY A. FOGDEN AND S. T. HYDE

Department of Applied Mathematics, Research School of Physical Sciences, Australian National University, Box 4, Canberra 2601, Australia

(*Received* 6 *June* 1991; *accepted* 10 *January* 1992)

Abstract

An explicit parametrization algorithm is reported for the simplest class of triply periodic minimal surfaces (the 'regular' class) for which the Weierstrass function specifying the complex plane representation has a simple product form. As the Gauss map links triply periodic minimal surfaces with spherical tessellations, the set of Schwarz triangular tilings of the sphere is used as the basis of an exhaustive listing of all such possible branch-point distributions, and hence surfaces, in this class. The symmetry and geometry of the resulting surfaces are determined by the locations and orders of these branch points.

1. Introduction

Minimal surfaces are the simplest members of the family of hyperbolic surfaces, which include all saddle-shaped (anticlastic) interfaces. If the surface is minimal, its principal curvatures are equal in magnitude and opposite in sign at all points on the surface. In contrast to the more familiar elliptic and parabolic geometries (which include spheres, ellipsoids, cylinders and planes*), a single hyperbolic surface may partition space into two continuous convoluted networks and the resulting geometry is known as a *bicontinuous* structure. The most symmetric examples of these structures are translationally ordered minimal surfaces. Such structures are to be found in molecular assemblies: thermotropic and lyotropic liquid crystalline phases and block copolymer phases and in the atomic arrays in microporous-framework alumino-silicates known as zeolites. At larger length scales these surfaces describe well the ultrastructure of biological mineral skeletons in some sea-urchins (Nissen, 1969). These interfaces are now of general interest to physicists, chemists and biologists (Dubois-Violette & Pansu, 1990).

Explicit mathematical realization of the surfaces in bicontinuous arrays is most simple for infinite (triply) periodic minimal surfaces (IPMS). Other hyperbolic interfaces (such as triply periodic constant-mean-curvature surfaces) can be related to their associated IPMS provided the topology of the interface is sufficiently complex (Anderson, Nitsche, Davis & Scriven, 1990). Five IPMS were discovered last century by Riemann and the school of Schwarz (see Riemann, 1953; Schwarz, 1890; Neovius, 1883). In the 1960s, Alan Schoen derived a number of new examples using soap films (Schoen, 1970); these cases have recently been confirmed by Karcher (1989). A large number of IPMS have also been found by Fischer & Koch (1989) and Koch & Fischer (1990) from crystallographic considerations.

In a series of three papers, we present techniques for systematic derivation and mathematical characterization of the simplest class of IPMS (which we shall term the 'regular' class), as well as some examples and general techniques for IPMS within the more general 'irregular' class. We characterize the various IPMS by the geometry of a *Flächenstück* of each surface, from which the infinite surface can be generated by reflection or rotation operations over the surface boundary.

* In fact, the plane can be classified as a minimal surface, albeit an uninteresting case.

0108-7673/92/040442-10$06.00

To derive these surfaces systematically and exhaustively, we resort to the Weierstrass parametrization of minimal surfaces, which defines the Cartesian coordinates of the surface (its global embedding in $\mathbf{R}^3$) by path integrals within the complex plane, which is the natural parameter domain for minimal surfaces. The 'regular' class admits of a simple closed form for the (complex) Weierstrass function generating the minimal surface, in terms of the branch-point positions and orders. The geometric and topological constraints of translational periodicity impose restrictions on these specifying quantities, thus permitting a complete listing of all IPMS in this class. In this paper we shall establish the mathematical groundwork for this parametrization scheme and derive the set of spherical tessellations which are the basis for the construction of these IPMS.

2. The Weierstrass representation of minimal surfaces

The study of minimal surfaces is greatly facilitated by the elegant parametrization due to Weierstrass, resulting from transformation of the surface into the complex plane by composition of two simple maps. The first is the Gauss map ν, under which the image of a point (x, y, z) of a surface $F(x, y, z) = 0$ is

$$(x', y', z') = \nabla F/|\nabla F|$$

[where $\nabla = (\partial/\partial x, \partial/\partial y, \partial/\partial z)$ is the gradient operator], the point of intersection of the surface normal vector at (x, y, z) with the unit sphere centred there. The second is stereographic projection σ of this sphere coordinate to the point

$$\omega = x'/(1-z') + iy'/(1-z')$$

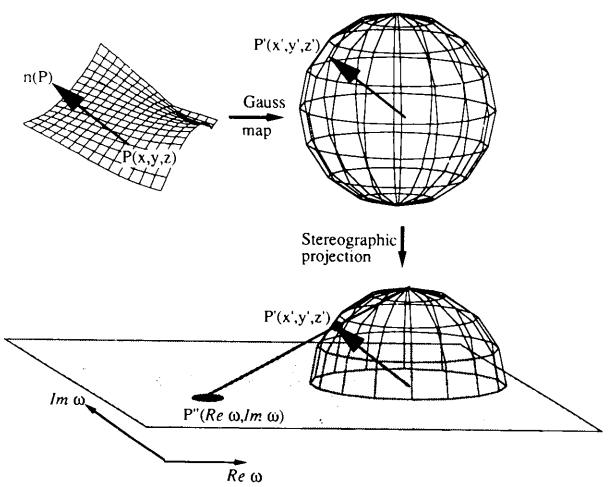

Fig. 1. The mapping of minimal surfaces into the complex plane. A point $P(x, y, z)$ on the surface (in $\mathbf{R}^3$) is mapped *via* its normal vector $\mathbf{n}$ onto the unit sphere [$P'(x', y', z')$] (the Gauss mapping). The sphere is then imaged onto the entire complex plane under stereographic projection, so that the complex coordinates of the point P are $P''(\mathrm{Re}\ \omega, \mathrm{Im}\ \omega)$.

in the complex plane $\mathbf{C}$ (Fig. 1). The composite map, $\sigma \circ \nu$, conformally maps the neighbourhood of any point of non-zero Gaussian curvature on the surface to a simply connected region of $\mathbf{C}$, on which its inverse $\Phi = \nu^{-1} \circ \sigma^{-1}$ was found by Weierstrass to be of the general form

$$\begin{aligned} x &= \mathrm{Re} \int_\omega (1-\omega'^2) R(\omega')\, \mathrm{d}\omega' \\ y &= \mathrm{Re} \int_\omega i(1+\omega'^2) R(\omega')\, \mathrm{d}\omega' \\ z &= \mathrm{Re} \int_\omega 2\omega' R(\omega')\, \mathrm{d}\omega' \end{aligned} \qquad (1)$$

(Re refers to the real part of the integrals) for some complex function $R(\omega)$ analytic in this region (Spivak, 1979). The Weierstrass function $R(\omega)$ completely specifies the first and second fundamental forms, and hence the differential geometry, of the surface. Most importantly, the Gaussian curvature of the surface at the point corresponding to ω is (Nitsche, 1975)

$$K = -4(1+|\omega|^2)^{-4} |R(\omega)|^{-2}. \qquad (2)$$

The local description (1) may be extended beyond a particular minimal surface patch by analytic continuation of the function $R(\omega)$ in the complex plane. As noted above, ω_i is a singular point of the continuation if its image $\Phi(\omega_i)$ is a point of zero Gaussian curvature (called a flat point) of the suface, in the vicinity of which the inverse Gauss map ν^{-1}, and hence Φ and R, is in general multivalued. Now the natural domain of (single-valued) definition of such a multivalued function $R(\omega)$ is its Riemann surface over $\mathbf{C}$, branched at $\{\omega_i\}$. Hence, if the integration range is defined to be the Riemann surface of the Weierstrass function, equations (1) represent a global parametrization of the minimal surface.

3. The Weierstrass function of an IPMS

An IPMS is characterized by its fundamental unit, from which the entire surface is generated by translation alone. As translation preserves normal directions, the surface is Gauss-mapped to an infinity of superpositions of the image of this unit. This image is the compact covering of the sphere corresponding to the Riemann surface of the Weierstrass function. The compactness of the Riemann surface over the unit sphere implies by a general result (Springer, 1957) that $R(\omega)$ is an algebraic function. Hence, with s denoting the (finite) number of sheets comprising the Riemann surface, the Weierstrass function is the solution of the sth-degree polynomial equation

$$\sum_{M=0}^{s} a_M(\omega) R^M = 0 \qquad (3)$$

for some set of polynomial functions $\{a_M(\omega)\}_{M=0}^{s}$.

(a) Local differential geometry

The form of an algebraic function is dictated by its singularity structure, which is evident here from simple considerations of the local differential geometry of the surface. In particular, at a member of the finite set of flat points on the fundamental unit of the IPMS, the angle of intersection of any two geodesics through this point is increased in the Gauss-map image by an integral factor $(b+1)$, termed the degree of the Gauss map at that point. This corresponds to a branch point of order b on the Riemann surface, at which the $(b+1)$ joined branches of the Weierstrass function diverge, by virtue of (2), as $a/(b+1)$ for some a coprime to $(b+1)$. Hence, with $\{\omega_i\}_{i=1}^n$ denoting the distinct flat-point normal-vector images, on a sheet of the Riemann surface pinned at a branch point, order b_i, under ω_i, the Weierstrass function has the asymptotic form

$$R(\omega) \sim \gamma_i(\omega-\omega_i)^{-a_i/(b_i+1)}, \qquad \omega \to \omega_i, \tag{4}$$

where γ_i is some complex constant. Furthermore, the Gaussian curvature of the surface is everywhere finite, so (2) implies $R(\omega)$ is non-zero on $\mathbf{C}$. Considering the closed complex plane, a suitable coordinate rotation (if necessary) will ensure that the point at infinity (the north pole of the Riemann sphere) is not a flat-point image, since the flat points are isolated. Then, from (2), the s branches of the Weierstrass function exhibit the common asymptotic form

$$R(\omega) \sim \gamma_\infty \omega^{-4}, \qquad \omega \to \infty \tag{5}$$

(for some set of s constants γ_∞) and hence the functions are analytic at infinity, as required.

(b) Topology

Additional conditions arise from the topological connection between the fundamental surface unit and its Gauss-map image, the Riemann surface over the unit sphere of the Weierstrass function (Hyde, 1989). The Euler characteristic of any compact connected orientable surface of genus g is given by

$$\chi = 2-2g.$$

Now the Riemann–Hurwitz formula states that the Euler characteristic of a Riemann surface is simply specified by its number of sheets, s, and total branch point order, W, as (Hopf, 1983)

$$\chi = 2s - W \tag{6}$$

or, equivalently,

$$g = 1 - s + \tfrac{1}{2}W.$$

Note that g is also the genus of the fundamental unit of the IPMS since the Gauss map is a homeomorphism between the two surfaces. The degree, d, of this map is the algebraic proportion of the unit sphere covered by the image. The simple relation

$$\chi = (1/2\pi) \iint_{\text{unit}} K \, dS \tag{7}$$

between the Euler characteristic and the integral curvature supplies the result (Hopf, 1983):

$$d = \tfrac{1}{2}\chi.$$

As the Gaussian curvature of a minimal surface is everywhere non-positive, the degree is the negative of the number of sheets of the Riemann surface, hence

$$\chi = -2s \tag{8}$$

or, equivalently,

$$g = s + 1$$

and (6) implies

$$W = 4s. \tag{9}$$

4. Regular class of IPMS

In this study, we limit detailed consideration to the class of IPMS for which each flat point has normal vector coincident only with those of other flat points exhibiting identical degeneracy on the surface. We refer to this as the 'regular' class since only locally equivalent flat points are superposed in the Gauss map, ensuring that its image is a regular multiple covering of the unit sphere. Hence, the resulting branch-point structure characterizing the Riemann surface is extremely simple. Above any flat-point image ω_i there lie only branch points of order b_i at which, by definition, b_i+1 sheets are pinned. Hence there are $s/(b_i+1)$ such points above ω_i (implying that s is a multiple of each b_i+1) and the total branch-point order is

$$W = s \sum_{i=1}^{n} b_i/(b_i+1).$$

Combining the above two equations, we get the constraint on the set of branch-point orders

$$\sum_{i=1}^{n} b_i/(b_i+1) = 4. \tag{10}$$

The implications of this assumption of 'regularity' on the Weierstrass function are addressed in the Appendix. It is found there that IPMS in this class possess the common Weierstrass functional form

$$R(\omega) = \exp(i\theta) \prod_{i=1}^{n} (\omega-\omega_i)^{-a_i/(b_i+1)} \tag{11}$$

[on scaling (x, y, z) with an appropriate real factor], subject to the constraint

$$\sum_{i=1}^{n} a_i/(b_i+1) = 4, \tag{12}$$

which on subtracting (10) implies

$$\sum_{i=1}^{n} (b_i - a_i)/(b_i + 1) = 0.$$

Now if $a_i > b_i$ for some i then the singularity of $R(\omega)$ at ω_i is non-integrable and the surface diverges to infinity. So true IPMS, for which the fundamental unit is compact, must satisfy $a_i \leq b_i$ for each i. The above equation then implies $a_i = b_i$ for each i, thus the general form of the Weierstrass function of an IPMS in the 'regular' class is now

$$R(\omega) = \exp(i\theta) \prod_{i=1}^{n} (\omega - \omega_i)^{-b_i/(b_i+1)}, \qquad (13)$$

subject to the constraint (10).

The isometric mapping of the minimal surface effected by the constant factor $\exp(i\theta)$ is referred to as the Bonnet transformation (Schoen, 1970; Hyde & Andersson, 1985). Attention is restricted in the most part here to the $\theta = 0$ surface (or the $\theta = \pi/2$ adjoint surface) in the family of Bonnet associates, given by the form

$$R(\omega) = \prod_{i=1}^{n} (\omega - \omega_i)^{-b_i/(b_i+1)}. \qquad (14)$$

While one is analysing the surface in the vicinity of a specific point, it is convenient to choose a coordinate orientation for which this point is mapped to the north pole of the unit sphere, projected to infinity in the closed complex plane. If the point is a flat point of the surface, say $\omega_n = \infty$, then the form (14) ceases to be appropriate and is replaced by

$$R(\omega) = \prod_{i=1}^{n-1} (\omega - \omega_i)^{-b_i/(b_i+1)}, \qquad (15)$$

subject to the previous constraint (10).

The above proof justifies the form (14) used by Lidin & Hyde (1987) to parametrize particular minimal surfaces in the 'regular' class. Conversely, it also states that any such surface must correspond to a Weierstrass function of this form and hence to a particular parameter set $\{\omega_i, b_i\}_{i=1}^{n}$. Hence (14) and (15) provide the basis of a systematic derivation of the 'regular' class of IPMS and enable explicit parametrization of those known members whose existence has only been verified empirically or numerically. The question of existence of minimal surfaces within the regular class can be resolved by consideration of the branch-point distribution in the complex plane, $\{\omega_i, b_i\}_{i=1}^{n}$, since this distribution completely determines the geometry of the minimal surface.

In the following two sections, we investigate the nature of fixed-point symmetries in minimal surfaces by analysis of the complex Weierstrass function that describes the surface.

5. Plane lines of curvature and linear asymptotes on IPMS

To each IPMS there corresponds a *Flächenstück* (surface element) from which the entire surface is generated by repeated analytic continuation across its boundaries. These bounding arcs may be taken to be geodesic curves of the surface. If a surface geodesic is a planar curve or straight line then it is referred to as a *plane line of curvature* or *linear asymptote*, respectively. These special geodesics are characteristic of reflection and rotation symmetries of a minimal surface. Plane lines of curvature lie in mirror planes of the complete minimal surface and linear asymptotes define twofold rotational axes* lying in the surface. The existence of plane lines of curvature and linear asymptotes may be readily established by analysing the behaviour of the Weierstrass function along such curves (Nitsche, 1975, p. 160). In this section we derive conditions on the branch-point distribution $\{\omega_i, b_i\}_{i=1}^{n}$ for a minimal surface specified by the functional form (14) or (15) to display these symmetries.

The family of geodesic curves passing through a particular point on the surface has a local Gauss-map image consisting of the great-circle arcs common to the corresponding point on the unit sphere, which form a common set of generic circular arcs in the complex plane under stereographic projection. (Note that the Weierstrass representation of a minimal surface is only defined up to rigid translation and rotation of the surface and a change of the complex variable parametrizing it.) For the specific representation (1), the conditions

$$(x, y, z)(\bar{\omega}) = \pm (x, -y, z)(\omega) \qquad (16)$$

constrain the real axis ($\mathrm{Im}\ \omega = 0$) to be the image of a line of curvature in the xz plane (positive sign), a mirror plane, or an asymptote along the y axis (negative sign), a twofold axis. These conditions reduce respectively to

$$R(\bar{\omega}) = \pm \bar{R}(\omega). \qquad (17)$$

In either case these functional constraints are satisfied by the form (14) [or its modified form (15) if a flat-point image resides at infinity in the closed complex plane] only if the sets of branch points of equal order are conjugate invariant, that is,

$$\{\bar{\omega}_i\} = \{\omega_i\}, \qquad b_i \text{ constant}. \qquad (18)$$

Mirror symmetry in the xz plane, or twofold rotational symmetry along the y axis, thus requires that this symmetry condition be obeyed by the branch points.

The presence of reflection planes or rotational axes in arbitrary directions on a minimal surface requires

* Note that higher-order rotational axes lying wholly in the surface cannot be present if the surface is free of self-intersections.

further analysis. For a general surface orientation, the boundary geodesics of interest map onto general great-circle arc images in the complex plane. To analyse such a geodesic with respect to the representation (1), consider an arbitrary great circle, defined by the plane through the sphere centre with normal $\hat{n} = (n_1, n_2, n_3)$ and corresponding to the circle $|n_3\omega + (n_1 + in_2)| = 1$ in projection. Apply the transformation

$$\begin{pmatrix} X \\ Y \\ Z \end{pmatrix}(w) = M \begin{pmatrix} x \\ y \\ z \end{pmatrix}[\omega(w)], \tag{19}$$

where

$$M = \begin{pmatrix} 1 - \dfrac{n_1^2}{1-n_2} & n_1 & \dfrac{-n_1 n_3}{1-n_2} \\ -n_1 & -n_2 & -n_3 \\ \dfrac{-n_1 n_3}{1-n_2} & n_3 & 1 - \dfrac{n_3^2}{1-n_2} \end{pmatrix}$$

and

$$\omega = \{-[n_1 - i(1-n_2)]w + n_3\}/\{n_3 w + [n_1 + i(1-n_2)]\}, \tag{20}$$

which describes the rotation of the surface and the unit sphere such that the plane of interest rotates into the XZ plane and the associated bilinear function maps the projected great-circle image onto the real axis (Im $w = 0$). Substitution of (1) and (20) into (19) yields

$$(X, Y, Z)(w) = \mathrm{Re} \int_w (1 - w'^2, i(1 + w'^2), 2w') \times \frac{[2(1-n_2)]^2}{\{n_3 w' + [n_1 + i(1-n_2)]\}^4} \times R\left(\frac{-[n_1 - i(1-n_2)]w' + n_3}{n_3 w' + [n_1 + i(1-n_2)]}\right) \mathrm{d}w'. \tag{21}$$

Then from (16) and (17), the conditions

$$(X, Y, Z)(\bar{w}) = \pm (X, -Y, Z)(w), \tag{22}$$

that an arc of the projected circle be the image of a line of curvature in the original plane (positive sign) or an asymptote directed along its normal line (negative sign), take the general form

$$\frac{1}{\{n_3\bar{w} + [n_1 + i(1-n_2)]\}^4} R\left(\frac{-[n_1 - i(1-n_2)]\bar{w} + n_3}{n_3\bar{w} + [n_1 + i(1-n_2)]}\right) = \pm \frac{1}{\{n_3\bar{w} + [n_1 - i(1-n_2)]\}^4} \times \bar{R}\left\{\frac{-[n_1 - i(1-n_2)w + n_3]}{n_3 w + [n_1 + i(1-n_2)]}\right\}. \tag{23}$$

For the Weierstrass function (14) [with accompanying condition (10)] to display this property, the constraint of conjugate invariance of the sets of transformed branch-point images of equal order,

$$\left\{\left(\overline{\frac{-[n_1 + i(1-n_2)]\omega_i + n_3}{n_3\omega_i + [n_1 - i(1-n_2)]}}\right)\right\} = \left\{\frac{-[n_1 + i(1-n_2)]\omega_i + n_3}{n_3\omega_i + [n_1 - i(1-n_2)]}\right\}, \qquad b_i \text{ constant}, \tag{24}$$

is now supplemented by the additional requirements

$$\prod_{i=1}^{n} \left(\frac{n_3\omega_i + [n_1 - i(1-n_2)]}{\overline{\{n_3\omega_i + [n_1 - i(1-n_2)]\}}}\right)^{b_i/(b_i+1)} = \pm 1 \tag{25}$$

or, equivalently,

$$\sum_{i=1}^{n} [b_i/(b_i+1)] \arg \{n_3\omega_i + [n_1 - i(1-n_2)]\} = \begin{cases} m\pi \text{ for plane lines of curvature} \\ (m + \frac{1}{2})\pi \text{ for linear asymptotes} \end{cases} \quad (m \in \mathbf{Z}). \tag{26}$$

This completes the analysis of twofold rotation axes and mirror planes in minimal surfaces of the regular class for which the Gaussian curvature is strictly negative at points whose normal vector is vertically upwards, *i.e.* which do not have a branch point at the point at infinity in the complete complex plane.

In the case of a branch point residing at infinity, say $\omega_n = \infty$, for which the modified Weierstrass form (15) is appropriate, consider separately the situations $n_3 \neq 0$ and $n_3 = 0$. In the former, equation (15) [again subject to (10)] likewise possesses the property (23) only if the conditions (24) and (25) or (26) apply, where in the limit $\omega_n \to \infty$ the index of the product and sum in (25) and (26) runs over the $(n-1)$ finite branch points $\omega_1, \ldots, \omega_{n-1}$ only. The latter is the degenerate case in which the great circle is projected to a ray through the origin in the complex plane, rotated clockwise through an angle φ from the real axis, where $\exp(i\varphi) = n_2 + in_1$. On substitution of (15) and (10) into (23), the analogue of the condition (24) is now

$$\{\overline{\exp(i\varphi)\omega_i}\} = \{\exp(i\varphi)\omega_i\}, \quad b_i \text{ constant}, \tag{27}$$

where only the finite branch points are considered (since the point at infinity is fixed in the transformation). Similarly (25) [or (26)] now assumes the form

$$\exp[i2\varphi(b_n + 2)/(b_n + 1)] = \pm 1 \tag{28}$$

or, equivalently,

$$\varphi = \begin{cases} [(b_n+1)/(b_n+2)]m\pi \\ \quad \text{for plane lines of curvature} \\ [(b_n+1)/(b_n+2)](m + \frac{1}{2})\pi \\ \quad \text{for linear asymptotes} \end{cases} \quad (m \in \mathbf{Z}). \tag{29}$$

Note there are $4(b_n+2)$ distinct permissible values of φ here (where $b_n \geq 0$ is the order of the branch point under consideration) since (b_n+1) and (b_n+2) are coprime, with the corresponding rays tracing the (b_n+1) sheets of the Riemann surface pinned there. Thus there are a maximum of (b_n+2) plane lines of curvature (or linear asymptotes), intersecting at angles equal to some multiple of $(b_n+2)^{-1}\pi$ at a flat point of order b_n on the minimal surface - a general result of differential geometry.

6. Perpendicular rotational symmetry

The existence of a rotational-symmetry axis through isolated points on the surface and normal to the surface may be examined in a similar manner. (Rotational axes inclined to the surface normal are indicative of self-intersections.) We use the transformed representation (21) for the case $n_3 = 0$ to seek rotation angles φ' about the Z axis through the point (whose image is projected to infinity) that maps the surface onto itself. Then the symmetry condition

$$(X, Y, Z)(w) = (x, y, z)(w) \qquad (30)$$

is fulfilled by the form (14) [or (15) if $b_n > 0$], subject to the constraint (10), only if the sets of finite branch points of equal order are invariant under the rotation, that is,

$$\{\exp(i\varphi')\omega_i\} = \{\omega_i\}, \qquad b_i \text{ constant}, \qquad (31)$$

and satisfy the additional equation

$$\exp[i\varphi'(b_n+2)/(b_n+1)] = 1, \qquad (32)$$

or, equivalently,

$$\varphi' = [(b_n+1)/(b_n+2)]2m'\pi \qquad (m' \in \mathbf{Z}). \quad (33)$$

Thus the minimal surface may exhibit perpendicular rotational symmetry at angles of some multiple of $(b_n+2)^{-1}2\pi$ about a flat point of order b_n, so the maximum rotational symmetry order in this case is (b_n+2), as expected. The connections between the order of a branch point and the symmetry of the resulting minimal surface is discussed in some detail elsewhere (Fischer & Koch, 1989).

On comparison of (29) and (33), it is clear that if the surface possesses plane lines of curvature (and/or linear asymptotes) then the angle of rotational symmetry is twice that of the intersection of these curves - a geometrically obvious general result. However, the converse does not apply in general. For the family of Bonnet associate surfaces, corresponding to multiplication of the Weierstrass function by the constant $\exp(i\theta)$, (22) is no longer satisfied while (30) is invariant. Hence, in this transformation, rotational symmetries are preserved in the absence of plane lines of curvature and linear asymptotes. [See, for example, the gyroid or G surface (Hyde & Andersson, 1985).]

In summary, the presence of reflection and rotation symmetries of the $\theta = 0$ (and $\theta = \pi/2$) surface with Weierstrass functional form (14) or (15) is related to the symmetries of the branch-point distribution in the complex plane.

So far we have not dealt with the question of translational periodicity of minimal surfaces in the regular class. In the final sections of this paper, we explore the range of branch-point distributions within this class that can lead to IPMS.

7. Spherical geodesic tessellating polygons

To generate an IPMS, the *Flächenstück* which builds the surface must lie within a cell that tiles three-dimensional Euclidean space [$\mathbf{R}^3$]. Consequently, the geodesic arcs bounding the *Flächenstück* are constrained to lie in the faces (or along the edges) of such a cell. Arcs of the $\theta = 0$ (or $\theta = \pi/2$) *Flächenstück* lying in planar faces or straight edges of the cell are plane lines of curvature or linear asymptotes, beyond which the surface (and its bounding cell) may be extended by mirror reflection or twofold rotation, respectively. (The surface is continued across arcs of the *Flächenstück* residing in curved faces or edges of the cell by a crystallographic operation involving translation, *i.e.* a screw rotation, glide reflection or pure translation.) Now consider bounding cells possessing at least one mirror plane or twofold axis. As the Gauss map of a plane line of curvature or linear asymptote is a great-circle segment, the image of such a *Flächenstück* is a continuous region of the Riemann surface over the unit sphere bounded by spherical geodesic arcs, which we call a generalized spherical geodesic polygon. This is immediately apparent in the case of a surface element entirely bounded by plane lines of curvature or linear asymptotes. More generally, the set of plane lines of curvature and/or linear asymptotes define a circuit under identification of curve-segment endpoints related by a translation-lattice vector of the IPMS and, since normal vectors are invariant on translation, the result still applies.

The operation of reflection (or rotation) of the *Flächenstück* in a bounding mirror plane (or about a bounding twofold axis) is then equivalent to reflection of the associated geodesic polygon on the unit sphere in the corresponding arc and thus to analytic continuation of the Weierstrass function to the region of its projected image in the complex plane. Repetition of this operation builds the fundamental translational unit of the IPMS and, in the process, the polygon tessellates the corresponding Gauss-map image of the fundamental unit; that is, the Riemann surface of the Weierstrass function over the unit sphere. Consequently, the *Flächenstück* must correspond to a tile of some number of sphere coverings. The branch-point structure is thus obtained from propagation of

the flat-point images in this geodesic polygon by the repeated reflections of the tessellation.

Clearly, the geometry of IPMS is intimately linked to the existence of tessellating polygons on the sphere. To generate IPMS in the regular class *via* their common Weierstrass functional form (14) or (15), consider spherical geodesic polygons that tessellate a finite number of copies of the unit sphere. Next, assign a branch-point set that, under the kaleidoscopic action of the tessellation, yields a distribution $\{\omega_i, b_i\}_{i=1}^{n}$ satisfying (10), subject to the regularity proviso that only branch points of the same order are superposed. Each such possible branch-point distribution must then be analysed to verify whether the Riemann surface of the resulting Weierstrass function may be constructed from the tessellation and, if so, whether this structure permits consistent identification of the congruence class of each polygon edge as the images of either plane lines of curvature or linear asymptotes. The pairs of equations necessary for a great-circle arc to be the image of such a curve are recalled and the appropriate requirement (24) or (27) (derived above) of branch-point symmetry is guaranteed for a distribution generated by a polygonal tessellation of the sphere; conditions (25) or (28) must then be satisfied for each arc in the family.

8. Schwarz triangle tessellations

A natural basis for tessellating polygons is the set of geodesic triangles which tile the sphere in a finite number of coverings. An exhaustive list of the fifteen basic triangles (one of which permits an infinity of subdivisions) was compiled last century by Schwarz (Erdélyi, Magnus, Oberhettinger & Tricomi, 1953).

Consider the encompassing set of derivative tilings which reduce to Schwarz cases on symmetric subdivision (*i.e.* triangulation) of the generating unit. The vocabulary of possible *Flächenstück* images is defined for each member of the set by the polygons comprising a finite union of tiles, which tessellate some number of copies of this underlying tiling and are assigned branch points according to the following convention. If the basis tiling admits of a subdivision, with respect to which the branch points on the polygon are related by a symmetry, then we refer the polygon to the subdivided Schwarz-case derivative. Conversely, if the tiling is a subdivision of another case from which the polygon may be constructed and the branch-point set is not symmetry-related on subdivision, then we analyse this situation with reference to the coarser tiling. This ensures that, on repeated reflection of the polygonal unit, the resulting branch-point distribution is identical for each sheet only if it is identical for each underlying tile. In this manner, the derivation of suitable branch-point distributions for IPMS in the regular class reduces to consideration of the permissible allocation of branch points to the single tile generating each Schwarz-case derivative. Furthermore, these points must then be propagated from one tile to its neighbours by symmetry operations of the tessellation – namely edge reflection or composition of this with reflection in any existing internal symmetry axes of the tile.

Table 1. *Schwarz tessellations corresponding to polyhedra*

Schwarz case	Vertex angles/π	Associated polyhedron
1	$\left(\frac{1}{2}, \frac{1}{2}, \frac{1}{n}\right)$	Dipyramids
	$\left(\frac{1}{2}, \frac{1}{2}, \frac{2}{n}\right)$	
2	$\left(\frac{1}{2}, \frac{1}{3}, \frac{1}{3}\right)$	Triakis octahedron
3	$\left(\frac{2}{3}, \frac{1}{3}, \frac{1}{3}\right)$	Triakis tetrahedron
4	$\left(\frac{1}{2}, \frac{1}{3}, \frac{1}{4}\right)$	Hexakis octahedron
5	$\left(\frac{2}{3}, \frac{1}{4}, \frac{1}{4}\right)$	Triakis hexahedron
6	$\left(\frac{1}{2}, \frac{1}{3}, \frac{1}{5}\right)$	Hexakis icosohedron
7	$\left(\frac{2}{5}, \frac{1}{3}, \frac{1}{3}\right)$	Triakis icosahedron
8	$\left(\frac{2}{3}, \frac{1}{5}, \frac{1}{5}\right)$	Pentakis dodecahedron
11	$\left(\frac{2}{5}, \frac{2}{5}, \frac{2}{5}\right)$	Icosahedron

All Schwarz cases for which the minimum number of coverings of the sphere by a tessellation exceeds one are then eliminated from consideration here, since they are incompatible with the regular class. The remaining cases are projections of the edges of standard polyhedra from their barycentres onto the concentric unit sphere.

The simplest case, with polar angles $(p/n)\pi$ dividing 2π, is the image of the family of dipyramids, composed of $2n/p$ isosceles triangles, in particular, $p/n = \frac{1}{2}$ corresponds to the octahedron. The other eight cases are the images of the eight regular or vertically regular polyhedra with triangular faces meeting at a common dihedral angle (Coxeter, 1973; Williams, 1979). This information is summarized in Table 1, with the tessellations categorized into the four Coxeter groups.

Within each such group, the first case listed is a subdivision of the other tilings, all of which have a vertex angle of the form $(2/n)\pi$, where n is an odd integer. After the assignment of an arbitrary set of branch points to the tile and symmetry operations of the tessellation to the two edges meeting at this vertex, consider the distribution thus generated on the $2n$ triangles on two sheets sharing the vertex. Pairs of superposed edges bear the same symmetry operation only if this is true of the generating edge pair, in

Table 2. *Branch-point solutions*

Here Φ denotes the empty set and the vertex-only solutions $\{\{b_j\}_{j=1}^3, \Phi, \Phi\}$ listed first in each case are abbreviated as $\{b_j\}_{j=1}^3$.

Case number	$(\lambda_1, \lambda_2, \lambda_3)$		$\{\{b_j\}_{j=1}^3, \{b'_k\}_{k=1}^{N'}, \{b''_l\}_{l=1}^{N''}\}$
1	$\left(\frac{1}{2}, \frac{1}{2}, \frac{1}{n}\right)$	n	
		2	$\{1, 2, 5\}; \{\Phi, \{1, 1\}, \Phi\}, \{\{0, 1, 1\}, \{1\}, \Phi\}, \{\{0, 0, 2\}, \{2\}, \Phi\}, \{\{0, 0, 1\}, \{3\}, \Phi\}; \{\Phi, \Phi, \{1\}\}$
		3	$\{0, 3, 7\}, \{0, 4, 4\}, \{0, 5, 3\}, \{0, 8, 2\}, \{1, 5, 0\}; \{\Phi, \{2\}, \Phi\}, \{\{0, 0, 1\}, \{1\}, \Phi\}$
		4	$\{0, 3, 1\}; \{\Phi, \{1\}, \Phi\}$
		5	$\{0, 1, 3\}, \{0, 4, 0\}$
		6	$\{0, 1, 1\}, \{0, 2, 0\}$
		8	$\{0, 1, 0\}$
4	$\left(\frac{1}{2}, \frac{1}{3}, \frac{1}{4}\right)$		$\{0, 1, 0\}, \{0, 0, 2\}$

which case the branch points on the two sheets are superposed only if the original set is symmetric with respect to the subdivision and hence permits analysis within the framework of the first case. Hence, of the fifteen Schwarz tessellations, only cases 1 (with polar angle π/n, $n \geq 2$), 2, 4 and 6 are consistent with the required regularity of the Gauss-map covering.

9. Branch-point distributions

Thus far, we have used the Schwarz tilings as a basis for determining the Riemann surface branch-point distributions which define Weierstrass functions of IPMS. Application of the remaining necessary condition (10) yields a finite set of possible such distributions for the regular class. This condition is formulated by calculating the number of distinct images, under the reflection operations generating the tessellation, of a branch point on a single tile that may, in general, reside in the interior or on one of the edges or vertices.

On consideration of a Schwarz spherical triangle, defined by vertex angles $(\lambda_1, \lambda_2, \lambda_3)\pi$, the Gauss-Bonnet theorem implies that the number F of tiles and the numbers E and V_j of edges and vertices of each type $j = 1, 2, 3$ per sheet in the resulting tessellation are given by

$$F = 8/\Lambda, \qquad E = 4/\Lambda, \qquad V_j = 4\lambda_j/\Lambda, \quad (34)$$

where

$$\Lambda = 2\left(\sum_{j=1}^{3} \lambda_j - 1\right). \quad (35)$$

Now let $\{b_j\}_{j=1}^3$, $\{b'_k\}_{k=1}^{N'}$ and $\{b''_l\}_{l=1}^{N''}$ denote the set of orders of the branch points distributed at the vertices $\{\lambda_j\pi\}_{j=1}^3$ and on the edges and face, respectively, of a single tile (where a zero order indicates absence of a branch point at that site). Equation (10) becomes

$$\sum_{j=1}^{3} V_j \frac{b_j}{b_j+1} + E \sum_{k=1}^{N'} \frac{b'_k}{b'_k+1} + F \sum_{l=1}^{N''} \frac{b''_l}{b''_l+1} = 4. \quad (36)$$

Insertion of (34) then gives the condition

$$\sum_{j=1}^{3} \lambda_j \frac{b_j}{b_j+1} + \sum_{k=1}^{N'} \frac{b'_k}{b'_k+1} + 2\sum_{l=1}^{N''} \frac{b''_l}{b''_l+1} = \Lambda, \quad (37)$$

reflecting the weighting of each branch-point contribution $b_i/(b_i+1)$ by the angles $\lambda_j\pi$, π or 2π, respectively, subtended by the tile at the point.

Hence each 'regular' IPMS generated by a Schwarz tiling of spherical triangles (as opposed to a derivative tiling thereof) corresponds to a non-negative integer set satisfying (37) for the case 1 (with polar angle π/n, $n \geq 2$), 2, 4 or 6. Determination of the solution sets in each case is straightforward. The fact that any positive integer b satisfies $\frac{1}{2} \leq b/(b+1) < 1$ yields bounds on the allowable numbers of each type of branch point and their respective orders, greatly simplifying the counting problem. For example, in case 4 of Table 1, (35) implies that $\Lambda = \frac{1}{6}$, and hence there can be no branch points at the $\pi/2$ vertices, on any edges or in any faces (*i.e.* $b_1 = b'_k = b''_l = 0$); accordingly (37) reduces to

$$4b_2/(b_2+1) + 3b_3/(b_3+1) = 2.$$

Likewise the possibility of branch points at both the $\pi/3$ and $\pi/4$ vertices is excluded (*i.e.* $b_2 = 0$ or $b_3 = 0$), leaving the two possibilities $b_2/(b_2+1) = \frac{1}{2}$ or $b_3/(b_3+1) = \frac{2}{3}$. As the solutions of these equations are integral (namely $b_2 = 1$ or $b_3 = 2$), they constitute the two permissible branch-point distributions for the Schwarz case 4. The exhaustive list of solution sets of (37) for all of these cases is given in Table 2. Note that no non-trivial solutions exist in cases 2 and 6 and in case 1 for $n = 7$ and $n \geq 9$.

Each of the solutions involving branch points on edges and/or faces yields a multiplicity of classes of possible IPMS given by the set of distinct allocations of the edge branch points and the choices of the (symmetry) operations defining the branch-point propagation over the three edges.

Concluding remarks

In this paper we have derived necessary conditions for a complex function to give rise to an IPMS in the 'regular' class *via* the Weierstrass equations. We have established that the question of existence of an IPMS in the regular class can be resolved by consideration of branch points alone. Strict constraints exist between the number and orders of the branch points specifying the complex (Weierstrass) function. Furthermore, the symmetries of the resulting IPMS can be deduced from the symmetries of the branch-point distribution, which are related to the underlying spherical tessellation.

In paper II of this series, we shall use these distributions to derive IPMS within the regular class explicitly and deduce the geometry and symmetries of the surfaces.

APPENDIX

The coefficient polynomials $a_M(\omega)$ in (3) can, without loss of generality, be expressed in the form

$$a_M(\omega) = \alpha_M P_M(\omega) \prod_{i=1}^{n} (\omega - \omega_i)^{q_{Mi}}, \qquad (A1)$$

in which any roots in the set $\{\omega_i\}_{i=1}^n$ are explicitly extracted. Hence $q_{Mi} \geq 0$ and the polynomial $P_M(\omega)$ is the product of all remaining factors of $a_M(\omega)$. Furthermore, we may assume that the constants α_s and α_0 are non-zero. It was noted in the text that $R(\omega)$ is necessarily non-zero on $\mathbf{C}$, hence we may assume that the polynomial $a_0(\omega)$ is likewise non-zero on $\mathbf{C}$ and thus $a_0(\omega) \equiv \alpha_0$. Also, the roots of the leading coefficient $a_s(\omega)$ are precisely the set of points $\{\omega_i\}_{i=1}^n$ above which the Riemann surface is branched, so $P_s(\omega) \equiv 1$ and $q_{si} \geq 1$.

As stated in the derivation of (5), no loss of generality results from assuming that the point at infinity in the closed complex plane is not a flat-point image and, moreover, that (3) yields s distinct values of the constant γ_∞. Hence the full polynomial degree must be preserved in the limit $\omega \to \infty$, implying that the first and last terms of the summation in (3) must be of equal asymptotic order (namely zero), with all intermediate terms of no larger (that is, positive) order. Now (5) and (A1) give the asymptotic forms

$$a_M(\omega) R^M \sim \alpha_M \gamma_\infty^M \omega^{(\deg P_M + \sum_{i=1}^n q_{Mi} - 4M)}, \qquad \omega \to \infty$$

(where deg P_M denotes the degree of the polynomial P_M), which thus impose the constraints

$$\sum_{i=1}^{n} q_{si} = 4s, \qquad (A2)$$

$$\sum_{i=1}^{n} q_{Mi} \leq 4M - \deg P_M, \qquad M = 1, \ldots, s-1. \qquad (A3)$$

We address the asymptotics at the flat-point images in an identical manner, now introducing the assumption of 'regularity'. Since only branch points, of order b_i, reside on the Riemann surface above ω_i, substitution of the asymptotic form (4) into (3) must result in s solutions for γ_i (counting with multiplicity). Hence as $\omega \to \omega_i$, again the first and last terms of the summation in (3) must be of equal order (zero) and all intermediate terms of no larger (that is, negative) order. Equations (4) and (A1) supply the asymptotics

$$a_M(\omega) R^M \sim \alpha_M \gamma_i^M P_M(\omega_i) \prod_{\substack{j=1 \\ j \neq i}}^{n} (\omega_i - \omega_j) \times (\omega - \omega_i)^{[q_{Mi} - Ma_i/(b_i+1)]}, \qquad \omega \to \omega_i$$

and thus the conditions

$$q_{si} = sa_i/(b_i+1), \qquad (A4)$$

$$q_{Mi} \geq Ma_i/(b_i+1), \qquad M = 1, \ldots, s-1. \qquad (A5)$$

Combination of (A2) and (A4) gives

$$\sum_{i=1}^{n} a_i/(b_i+1) = 4, \qquad (A6)$$

which in conjunction with the inequalities (A5) implies

$$\sum_{i=1}^{n} q_{Mi} \geq 4M, \qquad M = 1, \ldots, s-1. \qquad (A7)$$

Consistency between the inequalities (A3) and (A7) then demands

$$\deg P_M = 0 \Rightarrow P_M \equiv 1$$

and (A8)

$$\sum_{i=1}^{n} q_{Mi} = 4M, \qquad M = 0, \ldots, s,$$

from which (A5) and (A6) yield

$$q_{Mi} = Ma_i/(b_i+1), \qquad M = 0, \ldots, s. \qquad (A9)$$

Hence, *via* (A1), (A8) and (A9),

$$a_M(\omega) R^M = \alpha_M \left(\prod_{i=1}^{n} (\omega - \omega_i)^{a_i/(b_i+1)} R \right)^M,$$

so the defining equation (3) reduces to the constant-coefficient polynomial equation

$$\sum_{M=0}^{s} \alpha_M z^M = 0, \qquad z = \prod_{i=1}^{n} (\omega - \omega_i)^{a_i/(b_i+1)} R.$$

Thus z is a constant complex number and the Weierstrass function of an IPMS in the 'regular' class has the form

$$R(\omega) = z \prod_{i=1}^{n} (\omega - \omega_i)^{-a_i/(b_i+1)},$$

subject to the constraint (A6).

References

ANDERSON, D. M., NITSCHE, J. C. C., DAVIS, H. T. & SCRIVEN, L. E. (1990). *Adv. Chem. Phys.* **77**, 337.
COXETER, H. S. M. (1973). *Regular Polytopes.* New York: Dover.
DUBOIS-VIOLETTE, E. & PANSU, B. (1990). Editors. *J. Phys. (Paris) Colloq.* C7.
ERDÉLYI, A., MAGNUS, W., OBERHETTINGER, F. & TRICOMI, F. G. (1953). *Higher Transcendental Functions.* Bateman Manuscript Project. New York: McGraw-Hill.
FISCHER, W. & KOCH, E. (1989). *Acta Cryst.* A**45**, 726-732.
HOPF, H. (1983). *Differential Geometry in the Large. Springer Lecture Notes in Mathematics.* Berlin: Springer.
HYDE, S. T. (1989). *Z. Kristallogr.* **187**, 165-185.
HYDE, S. T. & ANDERSSON, S. (1985). *Z. Kristallogr.* **170**, 225-239.
KARCHER, H. (1989). *Manuscr. Math.* **64**, 291-337.
KOCH, E. & FISCHER, W. (1990). *Acta Cryst.* A**46**, 33-40.
LIDIN, S. & HYDE, S. T. (1987). *J. Phys. (Paris)*, **48**, 1585-1590.
NEOVIUS, E. R. (1883). *Bestimmung Zweier Speciellen Periodische Minimalflaechen.* Helsinki: Frenckel.
NISSEN, H.-U. (1969). *Science*, **166**, 1150-1152.
NITSCHE, J. C. C. (1975). *Vorlesungen über Minimalflächen.* Berlin: Springer Verlag.
RIEMANN, B. (1953). *Über die Fläche vom kleinsten Inhalt bei gegebener Begrenzung. Gesammelte Mathematische Werke.* New York: Dover.
SCHOEN, A. H. (1970). *Infinite Periodic Minimal Surfaces Without Self-intersections.* NASA Technical Note No. D5541, Washington, DC, USA.
SCHWARZ, H. A. (1890). *Gesammelte Mathematische Abhandlungen.* Berlin: Springer.
SPIVAK, M. (1979). *A Comprehensive Introduction to Differential Geometry.* Berkeley: Publish or Perish.
SPRINGER, G. (1957). *Introduction to Riemann Surfaces.* Reading, MA: Addison-Wesley.
WILLIAMS, R. (1979). *The Geometrical Foundation of Natural Structure.* New York: Dover.

Acta Cryst. (1992). A**48**, 451-456

Direct-Space Methods in Phase Extension and Phase Determination. I. Low-Density Elimination

BY M. SHIONO* AND M. M. WOOLFSON

Department of Physics, University of York, Heslington, York YO1 5DD, England

(*Received* 9 *August* 1991; *accepted* 10 *December* 1991)

Abstract

A density-modification procedure for phase extension and refinement is described which replaces all density less than one-fifth of the height of a light-atom peak by zero. Its effectiveness is demonstrated by applications to a small and a medium-size protein structure. With high-resolution data, for the small protein, it is possible to extend and refine from 3 to 1 Å with a mean phase error less than 30°. Successful phase extension from 4 Å is also possible. In general it is shown that phase extension to high resolution gives less error than extension to lower resolution. It has also been shown that for a small protein it is possible to obtain an *ab initio* solution of the structure by refining from a complete set of random phases for all reflexions.

The basis of direct methods

Most direct methods consist of mathematical procedures carried out in reciprocal space which are designed to produce sets of phases satisfying particular constraints. The first powerful and generally applicable direct methods were those based on the tangent formula, introduced by Karle & Hauptman (1956),

$$\tan\varphi(\mathbf{h}) = \left\{\sum_{\mathbf{k}} |E(\mathbf{k})E(\mathbf{h}-\mathbf{k})| \sin[\varphi(\mathbf{k})+\varphi(\mathbf{h}-\mathbf{k})]\right\} \times \left\{\sum_{\mathbf{k}} |E(\mathbf{k})E(\mathbf{h}-\mathbf{k})| \cos[\varphi(\mathbf{k})+\varphi(\mathbf{h}-\mathbf{k})]\right\}^{-1}. \quad (1)$$

Although the tangent formula was derived by Karle & Hauptman from algebraic and statistical considerations, it can be given a real-space physical interpretation. The phase given by the tangent formula is just that which would be obtained if an E map, calculated with current phase estimates, was squared and the phase, $\varphi(\mathbf{h})$, of the Fourier coefficient of index $\mathbf{h}$ of the squared map was taken.

The precursor of the tangent formula, the three-phase relationship

$$\varphi(\mathbf{h})-\varphi(\mathbf{k})-\varphi(\mathbf{h}-\mathbf{k}) \simeq 0 \text{ (modulo } 2\pi) \quad (2)$$

was derived by Cochran (1955) from the condition that a set of correct phases should give an electron density map for which $\int_V \rho^3 \, dV$ is a maximum. This condition, somewhat intuitive in origin, expresses the

* Present address: Department of Physics, Kyushu University, Hakozaki 6-chome, Higashi-ku, Fukuoka, Japan.

0108-7673/92/040451-06$06.00